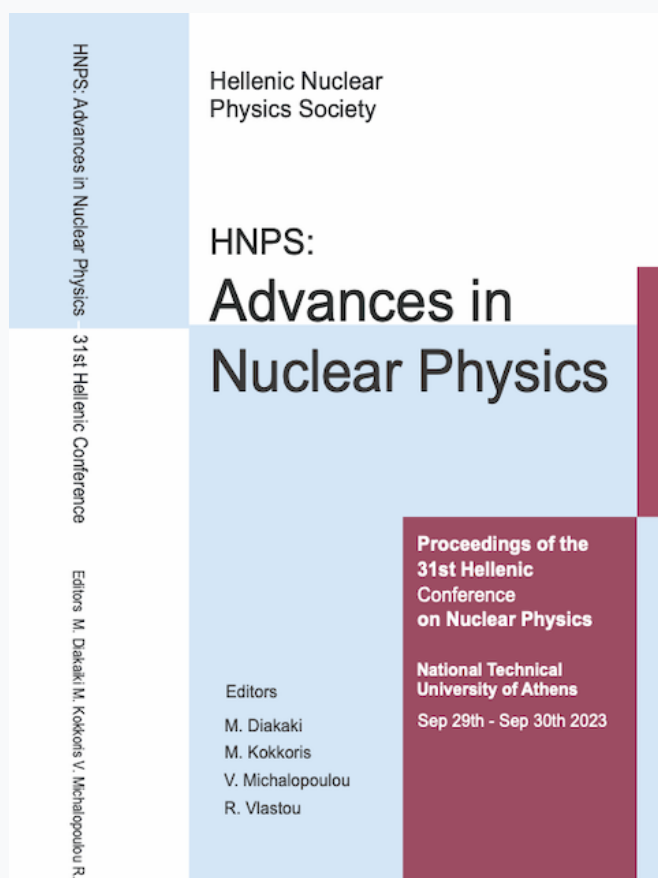


## HNPS Advances in Nuclear Physics

Vol 30 (2024)

HNPS2023



### Characterization of a Diamond, SiC and Si Detector Response to Neutron Beams at the NCSR “Demokritos”

*Kalliopi Kaperoni, Maria Diakaki, Mike Kokkoris, Christina Weiss, Erich Griesmayer, Julian Melbinger, Michail Axiotis, Sotiris Chasapoglou, Roza Vlastou, Theodor Fragner*

doi: [10.12681/hnpsanp.6389](https://doi.org/10.12681/hnpsanp.6389)

Copyright © 2024, Kalliopi Kaperoni, Maria Diakaki, Mike Kokkoris, Christina Weiss, Erich Griesmayer, Julian Melbinger, Michail Axiotis, Sotiris Chasapoglou, Roza Vlastou, Theodor Fragner



This work is licensed under a [Creative Commons Attribution-NonCommercial-NoDerivatives 4.0](https://creativecommons.org/licenses/by-nc-nd/4.0/).

### To cite this article:

Kaperoni, K., Diakaki, M., Kokkoris, M., Weiss, C., Griesmayer, E., Melbinger, J., Axiotis, M., Chasapoglou, S., Vlastou, R., & Fragner, T. (2024). Characterization of a Diamond, SiC and Si Detector Response to Neutron Beams at the NCSR “Demokritos”. *HNPS Advances in Nuclear Physics*, 30, 25–30. <https://doi.org/10.12681/hnpsanp.6389>

# Characterization of a Diamond, SiC and Si Detector Response to Neutron Beams at the NCSR “Demokritos”

K. Kaperoni<sup>1</sup>, M. Diakaki<sup>1</sup>, C. Weiss<sup>2,3</sup>, E. Griesmayer<sup>2,3</sup>, J. Melbinger<sup>2,3</sup>, M. Kokkoris<sup>1</sup>,  
M. Axiotis<sup>4</sup>, S. Chasapoglou<sup>1</sup>, T. Fragner<sup>3</sup>, R. Vlastou<sup>1</sup>,

<sup>1</sup> Department of Physics, National Technical University of Athens, Heroon Polytechniou 9,  
15780 Zografou, Greece

<sup>2</sup> TU Wien, Atominstytut, 1020 Wien, Austria

<sup>3</sup> CIVIDEC Instrumentation GmbH, 1010 Wien, Austria

<sup>4</sup> Tandem Accelerator Laboratory, Institute of Nuclear and Particle Physics “Demokritos”, 15341 Agia  
Paraskevi, Greece

---

**Abstract** Detecting low energy neutrons (below 6 MeV) can be a challenge mostly due to the high  $\gamma$ -ray contamination and the low efficiency of the detectors. Over the last years semiconductor neutron detectors have been developed and due to their unique characteristics, they have been proven useful in numerous applications. Diamond, SiC and Si are the most popular materials for constructing resilient semiconductor detectors. Diamond exhibits excellent physical and electrical properties and it is the material of choice when high energy resolution, irradiation resistance and hardness is required. Silicon (Si) is the most commonly used material for semiconductor detectors, used in microelectronics as well as in various radiation applications. In addition, SiC shows increased radiation resistance and over the last decades it is used for applications in harsh environments, including extreme temperatures and intense radiation conditions. There is also a great interest in studying SiC based semiconductors, since it is a new and promising material, currently not available in the market and the substrate thicknesses produced are very limited. In this work, a study was made with a Diamond a Si and a SiC detector to detect four low neutron energies: 2.45 MeV, 2.95 MeV, 3.45 MeV and 3.95 MeV, with quasi-monoenergetic neutron beams at the National Center for Scientific Research (NCSR) “Demokritos”. The experimental spectra were extracted, the calibration of the detectors used was performed and the elastic scattering spectrum was compared with the angular distribution.

**Keywords** Diamond, Si, SiC, Neutrons, Calibration

---

## INTRODUCTION

Wide band-gap semiconductor detectors are promising materials for many neutron applications, such as high energy experiments, fusion diagnostics, medical or space applications [1-4]. Materials with a large band-gap energy will have a low probability of thermal excitation and consequently will show a low leakage current in the detector. A significant advantage of the semiconductor detectors is their small size and weight compared to gas-filled detectors: due to the high density of a solid detection medium (almost 1000 times higher than for a gas-filled detector). As a result, they can collect the charged particles in much smaller volumes than those needed by scintillators or gas detectors. Semiconductor detectors are also characterized by fast response. Most of the semiconductor detectors are operated in a high electric field, resulting in saturated drift velocities for the ionization charge carriers, which are of the order of  $10^5$  m/s. This means that for dimensions of 100  $\mu\text{m}$  the time to collect the carriers will be under 10 ns [5].

Over the last years semiconductor-based neutron detectors receive considerable attention due to their low operating voltage, high energy resolution and radiation resistance. White neutron beams can be generated either by radioactive sources such as Pu-Be, by fission (in nuclear reactors), by accelerating electrons in a heavy target, producing bremsstrahlung radiation followed by photonuclear reactions ( $\gamma, n$ )/( $\gamma, f$ ), or by spallation, while monoenergetic neutron beams are produced through charged particle reactions such as ( $a, n$ ), ( $d, n$ ) or ( $p, n$ ). Most of these environments are accompanied by a high

$\gamma$ -ray background and intense radiation conditions. Therefore, an ideal semiconductor candidate must have first and foremost a high  $\gamma$ -rejection rate, also the ability to discriminate neutrons from  $\gamma$ -rays, fast response and resistance to high temperatures and harsh radiation conditions.

Diamond, SiC and Si are materials used for semiconductor neutron detectors able to perform under these conditions. Diamond has exceptional electrical and physical properties, the most notable being its high band-gap energy and thermal conductivity, which contribute to its low electronic noise, high energy resolution and irradiation resistance [6]. Due to the high strength of the Si-C bond, SiC, similar to Diamond, provides material advantages such as increased chemical and radiation endurance, making it ideal for use in harsh environments [7]. Silicon is a preferred material for neutron detection due to its low  $Z$  which results in low  $\gamma$ -ray interaction probability (Si has a higher  $\gamma$ -ray sensitivity than SiC which has higher  $\gamma$ -ray sensitivity than Diamond). Si also provides low manufacturing cost, and significant high technological know-how from the silicon-based microelectronics sector [8].

The detection of neutrons in such a detector depends on the neutron energy. For neutrons with energy higher than 6 MeV nuclear reactions such as (n,a), (n,p), (n,d) can be used. When a charged particle is produced it creates an isolated peak which can be easily distinguished from the noise and can be used for detailed analysis as well as for calibration. This is the case for 14 MeV (or higher energy) neutrons, which are extensively studied due to their interest for fusion (DT fusion), where a peak at  $\sim 8.4$  MeV is shown at a Diamond and SiC detector formed by the  $^{12}\text{C}(n,a)^9\text{Be}$  reaction [9,10]. With increasing neutron energy more reaction channels are open and thus more pronounced peaks can be observed. Similar for Si as well as SiC detectors due to the  $^{28}\text{Si}(n,a)^{25}\text{Mg}$  reaction a variety of distinguished peaks can be formed as shown in [11].

For neutrons with energy between approximately 1 MeV and 6 MeV the main interactions that occur with the C or Si nuclei is the elastic and inelastic scattering and the recoil nuclei can be detected. In this energy region detecting the produced neutrons can be a challenge due to both the  $\gamma$ -ray contamination, described above, and the low efficiency of the detectors. This leads to the lack of data in the literature for neutron energies below 6 MeV. In the following sections the performance of three different semiconductor detectors, Diamond, SiC and Si for four low neutron energies (2.45 MeV, 2.95 MeV, 3.45 MeV and 3.95 MeV) is described.

## EXPERIMENTAL DETAILS

The experiment was conducted at the neutron production facility of the Tandem accelerator at the Institute of Nuclear and Particle Physics (I.N.P.P.) of the National Center of Scientific Research (N.C.S.R.) "Demokritos". This facility generates quasi-monoenergetic neutron beams by the nuclear interactions of light ions with gaseous or solid targets. In our case, protons were impinging on a solid TiT target to generate neutron beams of 2.45, 2.95, 3.45, and 3.95 MeV, respectively. The proton energies used, the neutron energy, as well as the error in the neutron energy (calculated by simulations) are shown on Table 1. The proton beam, after its acceleration, interacts with the materials in the aluminum flange, where the solid TiT target is placed. The uncertainty in the proton beam energy is 1 keV per MeV. Inside the flange the protons first interact with a thin Mo foil with 10  $\mu\text{m}$  thickness followed by the main TiT target with 5.7  $\mu\text{m}$  thickness and then a thick Cu target with 1 mm thickness. The main neutron production occurs from (p,n) reactions with the  $^3\text{H}$  target, however (p,n) reactions may occur with Mo, Cu or Ti isotopes inside the flange, which can result in the production of parasitic neutrons. For the proton energies used the cross section of the secondary reactions is below 0.2 barns for these isotopes. Neutrons with lower energy than the main neutron beam can be produced from the surrounding materials of the target. With this process quasi-monoenergetic neutron beams are produced, with a main peak in the neutron energy of interest followed by a continuous distribution of parasitic neutrons, which extends to lower energies with low statistics.

The experimental set-up is shown in Figure 1. In this experiment a 50  $\mu\text{m}$  single-crystal CVD diamond detector, fabricated via the chemical vapor deposition technology, a 20  $\mu\text{m}$  4H-SiC and a 500  $\mu\text{m}$  Si sensor were tested, all of them with dimensions of 4 x 4 mm<sup>2</sup>. The sCVD Diamond, SiC and Si detectors were developed by CIVIDEC Instrumentation [12]. The sensor of each detector is packaged in a PCB (printed circuit board) structure consisting of FR4 (glass reinforced epoxy laminate material) metallized with Cu and Au.

**Table 1.** Proton energies used for the production of quasi-monoenergetic neutron beams at the NCSR “Demokritos”

Proton Energy (MeV)	Neutron Energy (MeV)	$\Delta E$ in Neutron Energy (MeV)
3.804	2.45	0.0612
4.256	2.95	0.0575
4.716	3.45	0.0542
5.128	3.95	0.0550

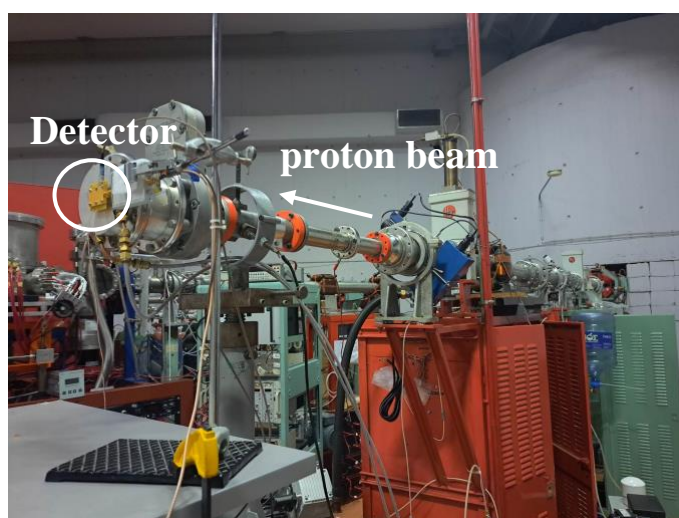


**Figure 1.** Experimental set-up of the NCSR “Demokritos”

The detectors were placed 12.8 mm away from the end of the flange at 0° with respect to the proton beam axis as shown in Figure 1. All the detectors were placed at the same position, centered with respect to the proton beam axis and consequently to the neutron beam, with an angular acceptance of  $\pm 10^\circ$ . Spectroscopic amplifiers from CIVIDEC Instrumentation [12] with a gain 12.5 mV/fC, and a gaussian pulse shape of 180 ns were used. The HV supply was inside the experimental area, placed 3 m away from the beam line. The sCVD diamond detector was operated at +50 V bias voltage ( $E = 1 \text{ V}/\mu\text{m}$ ), the SiC at +200V ( $E = 0.43 \text{ V}/\mu\text{m}$ ) and the Si at +80 V ( $E = 0.16 \text{ V}/\mu\text{m}$ ). The data was recorded with the CIVIDEC “ROSY” Readout System with 8 ns sampling period and 14-bit resolution.

## RESULTS AND DISCUSSION

The experimental spectra for the Diamond, SiC and Si detector for the neutron beams of 2.45, 2.95, 3.45, and 3.95 MeV are shown normalized to the peak at  $\sim 20$  channels for visualization purposes in Fig. 2. For these neutrons energies only the elastic scattering is possible with carbon nuclei in the case of Diamond, silicon nuclei in the case of Si and both in the case of SiC.

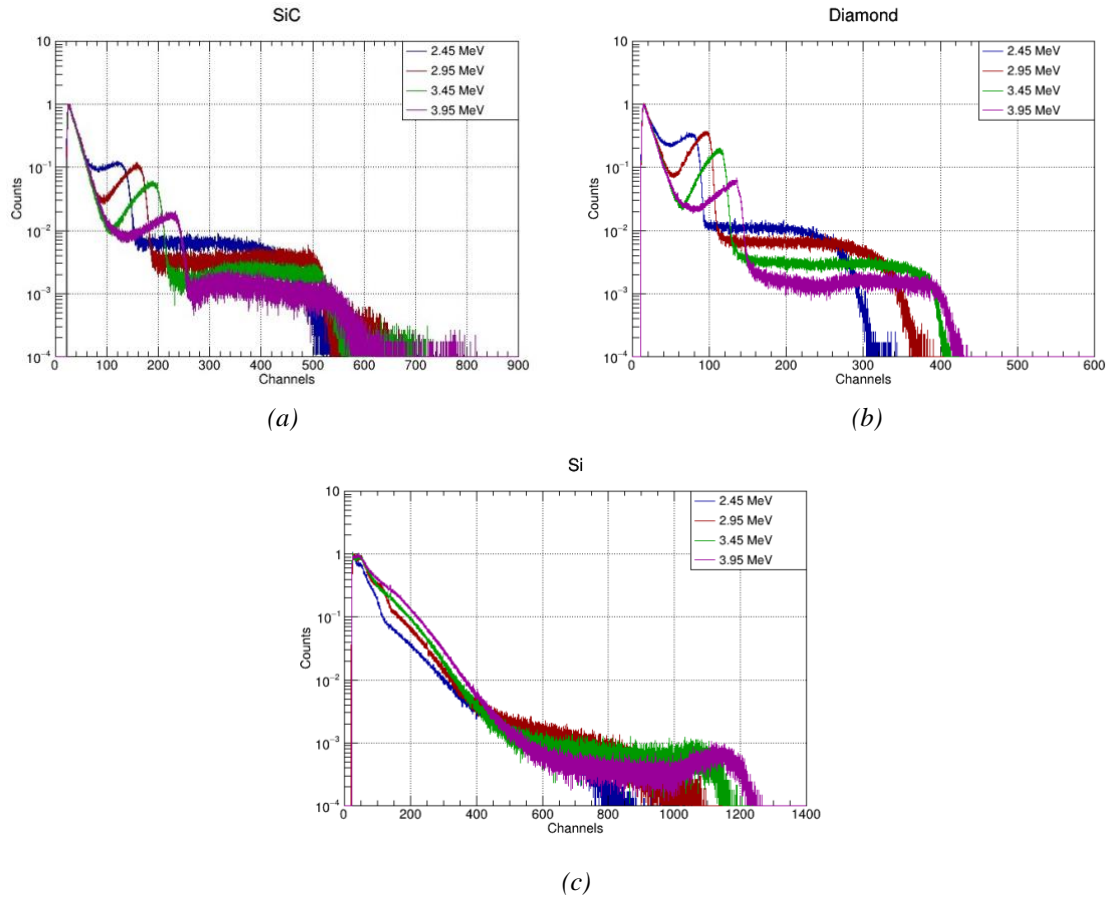


**Figure 2.** Experimental spectra of a 20  $\mu\text{m}$  SiC (a), a 50  $\mu\text{m}$  Diamond (b) and a 500  $\mu\text{m}$  Si detector (c)

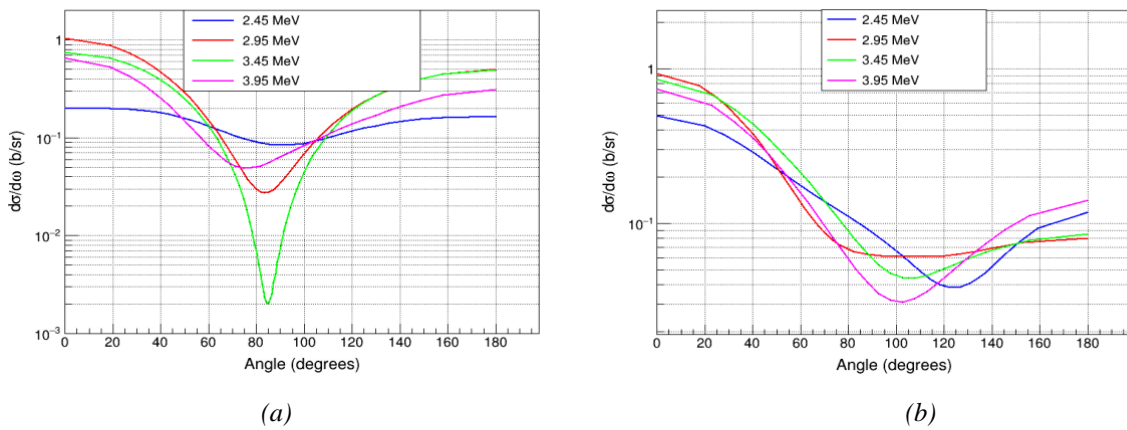


**Figure 3.** Angular distribution of neutron elastic scattering with (a)  $^{12}\text{C}$  and (b)  $^{28}\text{Si}$ . Data obtained from the ENDF/B-VIII.0 library [13].

In the Diamond detector the characteristic shape of the angular distribution of the neutron elastic scattering with  $^{12}\text{C}$  was observed, as shown in Figure 3(a), which is similar for SiC due to the presence of  $^{12}\text{C}$ . Also, the elastic scattering cut-off, which is the maximum energy the neutrons can transfer to the recoil nuclei, when the former is scattered at  $180^\circ$ , is clearly shown in both SiC and Diamond spectra.

In the experimental spectra of Diamond and SiC we also observe a plateau area which seems to start above the elastic scattering cut-off and extends to higher channels until it drops. This area is caused by the (n,p) reactions occurring in the PCB layer of the detectors and it is present at all the spectra. More specifically the incoming neutrons interact with the Hydrogen inside the FR4 layer through

$^1\text{H}(n,p)$ , resulting in a high-energy tail in the experimental spectra which is called proton recoil region. For Diamond and SiC the distinction between the elastic scattering, the characteristic cut-off and the proton recoil region is clear, which can lead to a successful neutron detection. Also, the  $\gamma$ -rays contamination is expected in the low energy region as shown in [14].

However, this is not the case for the Si detector. The shape of the angular distribution of the elastic scattering of  $^{28}\text{Si}$ , shown in Figure 3(b), differs from the  $^{12}\text{C}$  in the high scattering angles (above  $90^\circ$ ), which leads to a higher probability for scattered recoil nuclei in the low energy region (lower scattering angles result in lower energy transfer in the recoil nuclei). Consequently, due to the shape of the angular distribution, the lower elastic scattering cut-off (in comparison to  $^{12}\text{C}$ ) and the thickness of the sensor we cannot distinguish between Si recoils and proton recoils. In addition, due to the  $\gamma$ -rays background the recorded counts below  $\sim 0.3$  MeV are considered highly contaminated with  $\gamma$ -rays and cannot be resolved [14], so no clear distinction can be observed for the recoil  $^{28}\text{Si}$  nuclei for the neutron energies used.

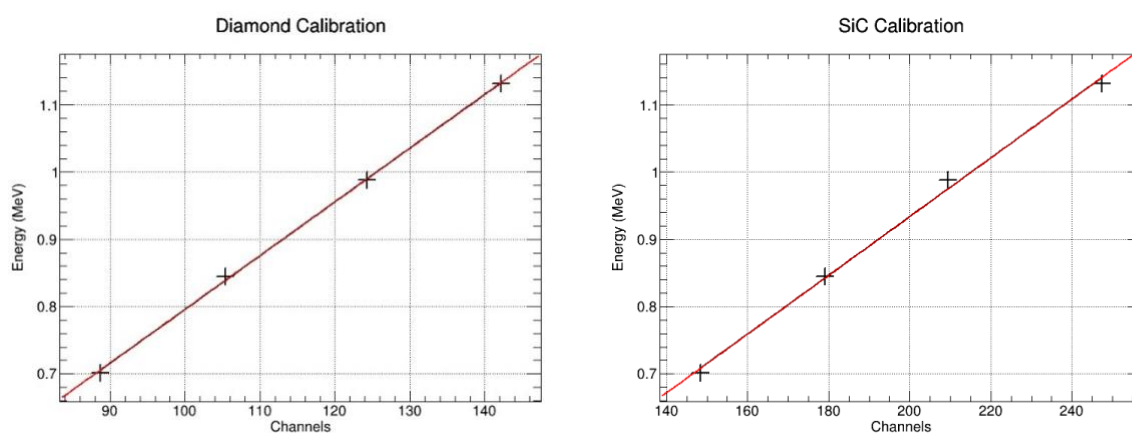


**Figure 4.** Preliminary calibration of the 50  $\mu\text{m}$  Diamond detector (left) and the 20  $\mu\text{m}$  SiC detector (right)

Using  $^{12}\text{C}$  neutron elastic scattering cut-off for all the neutron beams, the calibration of the Diamond and SiC detector can take place. The calibration of the Diamond and SiC detector is shown in Figure 4. The elastic scattering cut-off for 2.45, 2.95, 3.45, and 3.95 MeV neutrons on  $^{12}\text{C}$  is 0.702, 0.845, 0.988, and 1.132 MeV, respectively. We observe that the calibration shows a linear behavior for the Diamond and SiC detector, which shows the linearity of the amplifiers. Via SRIM calculations it was found that for the 50  $\mu\text{m}$  Diamond sensor the proton recoils for 2.45 and 2.95 MeV neutrons can be stopped and deposit their full energy in the detector volume, but for the 20  $\mu\text{m}$  SiC none of the recoils can be stopped. The thickness of both sensors and the calibration points that can be used are under investigation. Further analysis for this work is ongoing.

## CONCLUSIONS

In this work the study of a 50  $\mu\text{m}$  Diamond, 20  $\mu\text{m}$  SiC and 500  $\mu\text{m}$  Si detector was made for four quasi-monoenergetic neutron beams of 2.45, 2.95, 3.45, and 3.95 MeV, produced in the Tandem accelerator at the I.N.P.P. of the NCSR "Demokritos". Since most studies are focused in measuring high energy neutrons (above 6 MeV) where secondary reactions channels are open, detecting these low energy neutrons through elastic scattering can be a challenge. The experimental spectra for the three detectors are presented and discussed and their shape is compared to the angular distribution of the neutron elastic scattering with  $^{12}\text{C}$  and  $^{28}\text{Si}$  nuclei. Due to the  $\gamma$ -rays contamination and the shape of the elastic scattering, it was determined that the Si detector is not able to clearly distinguish the recorded neutrons from the  $\gamma$ -rays and the proton recoils. However, both Diamond and SiC detector show

promising results and their calibration could be performed. Further analysis must follow this work including an investigation of the proton recoil region, a threshold to eliminate the  $\gamma$ -rays background as well as the extraction of the efficiency through analytic simulations.

### Acknowledgments

This work is supported by the Basic Research Program PEVE 2021 of the National Technical University of Athens and by CIVIDEC Instrumentation. Furthermore, this work was highly supported and encouraged by all the members of the NTUA nuclear physics group and our colleagues from the NCSR “Demokritos” in many different ways.

### References

- [1] L. Bertalot et al., JINST 7, C04012 (2012); doi: 10.1088/1748-0221/7/04/C04012
- [2] T. Matsumoto et al., NIM B 542, 151-157 (2023); doi: 10.1016/j.nimb.2023.06.013
- [3] T.P. Dachev et al., Life Sci Space Res 39, 43-51 (2023); doi: 10.1016/j.lssr.2023.01.001
- [4] T. Shimaoka et al., Functional Diamond 1, 205 (2021); doi:10.1080/26941112.2021.2017758
- [5] Glenn F. Knoll, Radiation detection and measurement, John Wiley & Sons (2010)
- [6] M. Angelone and C. Verona, J. Nucl. Eng. 2, 422 (2021); doi: 10.3390/jne2040032
- [7] F. Nava et al., Meas. Sci. Technol. 19, 102001 (2008); doi: 10.1088/0957-0233/19/10/102001
- [8] M. Tilli and A. Haapalinna, Handbook of Silicon Based MEMS Materials and Technologies, Chapter 1, 3–16 (2015); doi: 10.1016/B978-0-323-29965-7.00001-4
- [9] O. Obraztsova et al., IEEE Trans. Nucl. Sci. 65, 2380 (2018); doi: 10.1109/TNS.2018.2848469
- [10] M. Pillon et al., NIM A 640, 185 (2011); doi: 10.1016/j.nima.2011.03.005
- [11] F. Franceschini and F.H. Ruddy, Properties and Applications of Silicon Carbide, Chapter 13 (2011); doi: 10.5772/15666
- [12] Detectors, CIVIDEC Instrumentation, Vienna, Austria, Retrieved from: <https://cividec.at/>
- [13] Evaluated Nuclear Data File, Retrieved from: <https://www-nds.iaea.org/exfor/endl.htm>
- [14] K. Kaperoni et al., HNPS Adv. Nucl. Phys. 29, 58 (2023); doi: 10.12681/hnpsanp.5184